Cerrahpaşa Med J 2023; 47(2): 141-149 ORIGINAL ARTICLE

Value of Fluoro-2-Deoxy-D-Glucosefluoro-2-Deoxy-D-Glucose Positron Emission Tomography/Computed Tomography in Symptomatic and Asymptomatic Tuberculosis

Elife Akgün[1], Reşit Akyel[2]

[1]Department of Nuclear Medicine, University of Health Sciences Turkey, Başakşehir Çam and Sakura City Hospital, İstanbul, Turkey
[2]Department of Nuclear Medicine, University of Health Sciences Turkey, Yedikule Pulmonary Diseases and Thoracic Surgery Training and Research Hospital, İstanbul, Turkey

Cite this article as: Akgün E, Akyel R. Value of 18-fluorine fluoro-2-deoxy-d-glucose–positron emission tomography/computed tomography in symptomatic and asymptomatic tuberculosis. *Cerrahpaşa Med J.* 2023;47(2):141-149.

Abstract

Objective: The aim of this retrospective study is to evaluate the difference of 18-fluorine fluoro-2-deoxy-D-glucose positron emission tomography/computed tomography images between the symptomatic and asymptomatic tuberculosis cases.

Methods: Patients diagnosed with tuberculosis underwent 18-fluorine fluoro-2-deoxy-D-glucose positron emission tomography/computed tomography imaging. Cases were categorized according to symptom status, types/number of symptoms, types/localization of lung lesions, and extrapulmonary involvement sides. Every lesion with pathologic features on computed tomography and/or increased 18-fluorine fluoro-2-deoxy-D-glucose uptake was measured semiquantitatively using the maximum standardized uptake value.

Results: One hundred fourteen patients (n = 40 female, n = 74 male; median age 57) were enrolled in this study. Although lung parenchyma involvement was observed significantly at a higher rate in males than females, pleural and lymph node involvement was revealed at significantly higher rates in females. No significant difference was found between the symptom-positive and -negative groups in terms of gender, localization/types of lung lesion, and extrapulmonary involvement sides detected with positron emission tomography/computed tomography. Based on the criteria of maximum standardized uptake value greater than 2.0 to define active lesions, 9.5% of symptomatic cases had inactive lesions, while 80% of asymptomatic cases had active lesions. There was no statistically significant difference between the maximum standardized uptake value values of the types of lung lesions. While a positive low correlation was detected between maximum standardized uptake value of lung parenchymal lesions and the number of symptoms, a negative moderate correlation was found between the maximum standardized uptake value values of the pleura and the age.

Conclusion: Interestingly, there was no significant difference between symptomatic and asymptomatic tuberculosis cases in terms of types of lung lesions and extrapulmonary involvement sides. The majority of the asymptomatic cases had active disease. Based on the findings, we think that 18-fluorine fluoro-2-deoxy-D-glucose, positron emission tomography/computed tomography is a valuable imaging modality even in asymptomatic cases with a low probability of clinically active tuberculosis.

Keywords: Fluorodeoxyglucose, PET/CT, pulmonary, tuberculosis

Introduction

Tuberculosis (TB) caused by *Mycobacterium tuberculosis* (*M. Tbc.*), is a contagious infectious disease, which is the leading cause of death worldwide.[1] Although it is a curable and preventable disease, about one-quarter of the world population is estimated to be latently infected with *M. Tbc.*[1,2] It is a slow-growing, highly aerobic bacteria primarily that affect the lung (in about 90% of cases),[3,4] but extrapulmonary (EP) TB can also occur especially in immunosuppressed patients.

Decreased desire to eat, decrease in body weight, sweating especially at night, high fever, and cough accompanied by hemoptysis lasting more than 3 weeks are among the typical symptoms of tuberculosis. However, different symptoms can be seen depending on which part of the body is involved.

Received: February 26, 2023 **Accepted:** April 4, 2023
Publication Date: August 22, 2023
Corresponding author: Elife Akgün, Department of Nuclear Medicine, University of Health Sciences Turkey, Başakşehir Çam and Sakura City Hospital, İstanbul, Turkey
e-mail: elifekaymak@hotmail.com
DOI: 10.5152/cjm.2023.23013

18-Fluorine fluoro-2-deoxy-D-glucose positron emission tomography/computed tomography (18-F FDG PET/CT) can be used for more than 1 indication. The most important area of use is the detection of oncological pathologies; however, its use in inflammatory events is becoming increasingly common. Macrophages and lymphocytes are the main cause of the inflammatory process seen in TB. 18-Fluorine fluoro-2-deoxy-D-glucose is also used as an imaging modality in TB by accumulating in these cells, which play an active role in immunity.[5] Together with the pulmonary (P) and EP involvement sides, it plays an important role in staging as well as in early diagnosis. Moreover, it provides important information in predicting the prognosis and choosing the most appropriate biopsy site.

The aim of this retrospective study is to evaluate the contribution of patients' symptoms with metabolic character of lesions that were detected with FDG PET.

Methods

Study Population

One hundred fourteen patients with a diagnosis of TB and who underwent FDG PET/CT with lung cancer malignancy suspicion

were included in this retrospective study. While the diagnosis can be made with clinical imaging, the presence of TB can also be revealed by bacteriological or histopathological examinations.

All clinical data of patients were recorded, including gender, age, status, number, and types of symptoms (sputum, cough, weight loss, tiredness, fever, hemoptysis, pain, night sweat, and dyspnea).

All procedures performed in studies involving human participants were in accordance with the ethical standards of the 1964 Helsinki Declaration. Due to the retrospective nature of this study, individual written consent was not necessary.

Patient Imaging and Positron Emission Tomography/Computed Tomography Data Analysis

Patients were injected with 3.7 MBq/kg of 18-F FDG after fasting for at least 6 hours with blood glucose level <180 mg/dL and scanned approximately 60 minutes after injection on PET/CT scanners (Discovery 600, GE Medical Systems, Milwaukee, Wis, USA). Computed tomography scanning was first acquired using a low dose technique (120 kVp, 250 mA, rotation time of 0.8 seconds, and 27.50 mm^2/rotation with DFOV 70 mm) without contrast agent injection and a PET scan was obtained immediately after the CT scan. Positron emission tomography scan acquisition time was 2 minutes per bed position. Scans were conducted from the middle of the thigh to the top of the skull. Attenuation correction was performed on the PET images using the corresponding CT images.

Areas of increased uptake were assessed qualitatively by visual analysis and semiquantitatively using the measurement of the standardized uptake value (*SUV*) of the involved sites. Standardized uptake value is calculated either as the ratio of tissue radioactivity concentration and the injected dose adjusted by body weight. The maximum *SUV* (*SUV*max) is obtained for a 1-pixel regions of interest corresponding to the maximum pixel value in the tumor.

Positron emission tomography/computed tomography images were analyzed by 2 experienced nuclear medicine specialists who were blinded to patients' clinicopathologic informations on a dedicated processing workstation (Advantage Window; GE Healthcare, Milwaukee, Wis, USA).

Any lesions with increased 18-F FDG uptake more than the surrounding tissue and/or showed pathologic features on CT images were considered positive for the involvement of TB. If there were multiple hypermetabolic P and/or EP lesions, in each category the lesion with the highest *SUV*max was selected. Patients were considered to have active lesions if their 18-F FDG PET images revealed a lesion with *SUV*max above 2 mg/dL.

When CT scan findings were evaluated, especially in the thoracic region, nodules (including micro), lymph nodes (including mediastinal and hilar), and areas of consolidation were noted for categorization. In addition, in the EP region, involvement of nonthoracic lymph nodes, intestinal organs (such as liver and spleen), peritoneum, bone, and soft tissue was also noted. Both mediastinal and lung windows were used in order to obtain maximum accuracy in the measurements.

Statistical Analysis

Data are presented as medians with extreme ranges. All the variables were assessed for normality by Kolmogorov–Smirnov test. For testing significance of difference in categorical variables between the 2 groups, Mann–Whitney *U*-test was used. Kruskal–Wallis test was used for testing the significance of any difference in PET parameters across the groups (symptom number, localization, and type of lung lesions). In case of a significant difference in Kruskal–Wallis test result, the categories were compared with the posthoc test (Bonferroni correction). The associations between PET parameters and symptom numbers/age/localization and type of lung lesions were calculated using Spearman test. A P value <.05 was considered statistically significant. All statistical analyses were performed using Statistical Package for Social Sciences version 22.0 (IBM SPSS Corp.; Armonk, NY, USA).

Results

One hundred fourteen patients with a TB history (n = 40 female, n = 74 male; median age 57, range 20-87 years) were included. Tuberculosis diagnoses were confirmed with PCR test and/or acid-fast bacilli positive at the sputum in 80% of cases, with TB culture in 60% of cases, and basis on clinic/radiologic findings in 10% of cases. Median age in males was significantly higher than in females (58.5 vs. 49; P = .001). Although lung parenchyma involvement was observed at a significantly higher rate in males than females (87.8% vs. 60%; P = .001), pleural involvement and mediastinal supraclavicular, and intraabdominal lymph node (LN) have revealed significantly higher rates in females than males (40% vs. 20.3%; P = .02, 70% vs. 47.3%; P = .02, 37.5% vs. 13.5%; P = .003, 32.5% vs. 12.2%; P = .009, respectively). When other clinical characteristics and imaging findings were evaluated, no significant difference was found between genders. More information about the clinical and PET/CT imaging data of the cohort is shown in Table 1.

The symptomatic group included 84 patients experiencing TB toxic symptoms or infection symptoms. Only 35 (41.7%) of 84 symptom-positive cases had 1 symptom; the remaining presented with multi-symptom. The asymptomatic group included 30 cases who mostly underwent FDG PET imaging for metabolic characterization of lung lesions. No significant difference was found between the symptom-positive and -negative groups in terms of gender, lung lesion localization, lung lesion types, and EP TB involvement sides detected with PET/CT.

Based on the criteria of *SUV*max greater than 2.0 to define active lesions, PET/CT showed abnormal lesions with increased metabolism, consistent with active disease in 100 patients (87.7%). While 80% (n = 24) of asymptomatic cases might have active lesions, 5% (n = 8) of symptomatic cases might have inactive lesions. Of the 100 cases of active TB, 25 were diagnosed with EP TB.

Focal FDG avidity in the skeletal system with no changes on CT images, suggesting marrow lesions, was seen in 6 cases. In 4 cases, hypermetabolic bone lesions were consistent with spondylodiscitis. No lung lesion was detected in 4 of 9 cases with bone involvement. In 2/9 cases liver and in 1/9 cases, spleen involvements were detected, and all of these cases were complicated with bone lesions.

The lesions of the patients with lung involvement were located in the upper lobe (n = 43, 48.3%), middle lobe (n = 3, 3.4%), lower lobe (n = 6, 6.7%), and multilobes (n = 37, 41.6%).

Maximum standardized uptake values of lesions located in the multilobar lung (n = 37) were significantly higher than lesions located in the superior lobe (n = 43) (7.24 g/mL vs. 4.52 g/mL, P = .002).

Although the highest *SUV*max value was measured from the lesion areas in the consolidation category (6.44 g/mL), there was no statistically significant difference between the *SUV*max values of the types of lung lesions (P = .09).

Maximum standardized uptake values of the lesions from the 18-F FDG PET/CT are summarized in Table 2.

While statistically significant positive low correlation was detected between *SUV*max of lung parenchymal lesions and the number of symptoms (r = 0.25, P = .02), a statistically significant moderate negative correlation was found between the *SUV*max

Table 1. The Relationship Between the Characteristics of the Patients and the Maximum Standardized Uptake Values of the Pathological Lesions

Variables		Lung Parenchyma, Median (Range) n	*P*	Pleural, Median (Range) n	*P*	Pleural Effusion, Median (Range) n	*P*	Mediastinal LN, Median (Range) n	*P*	Supraclavicular LN, Median (Range) n	*P*	Intraabdominal LN, Median (Range) n	*P*	Peritoneum, Median (Range) n	*P*	Bone, Median (Range) n	*P*
Gender	Female	6.6 (1.5-20.0) 24	.04*	12.0 (2.4-21.9) 16	.24	1.8 (1.2-3.4) 12	.55	6.8 (1.2-19.6) 28	.80	8.7 (3.4-25.2) 15	.74	6.3 (4.5-18.2) 9	0.57	6.2 (2.8-9.5) 2	.44	16.7 (11.6-23.5) 3	.21
	Male	4.8 (0.0-19.0) 65		5.6 (1.1-20.4) 15		1.6 (1.3-3.1) 14		7.3 (2.1-21.4) 35		6.9 (2.5-15.8) 10		7.8 (4.9-21.3) 13		9.4 (9.2-9.7) 2		14.0 (6.0-16.2) 7	
Symptom	(+)	4.9 (20.0-1.0) 64	.31	8.5 (1.1-21.9) 26	.26	1.7 (1.3-3.4) 23	.47	7.3 (2.1-21.4) 47	.75	8.1 (2.5-18.8) 20	.79	7.9 (4.9-21.3) 19	0.06	9.3 (2.8-9.7) 4	—	14.1 (6.0-16.7) 7	.73
	(–)	4.4 (0.0-12.3) 25		9.6 (2.0-13.9) 5		1.4 (1.2-2.4) 3		6.7 (1.2-21.1) 16		7.0 (4.0-25.2) 5		5.5 (4.5-6.3) 3		0		14.0 (11.6-23.5) 3	
Sputum	(+)	6.4 (1.3-20.0) 19	.03*	4.6 (1.1-20.4) 4	.20	1.4 (1.3-2.2) 5	.13	6.8 (2.1-19.2) 13	.21	6.9 (3.5-12.1) 6	.23	6.5 (5.7-18.2) 4	0.80	0	—	14.7 1	.60
	(–)	4.6 (0.0-12.3) 70		9.6 (1.7-21.9) 27		1.8 (1.2-3.4) 21		7.1 (1.2-21.4) 50		8.7 (2.5-25.2) 19		7.3 (4.5-21.3) 18		9.3 (2.8-9.7) 4		13.9 (6.0-23.5) 9	
Cough	(+)	5.3 (1.2-19.0) 33	.25	7.5 (1.1-21.9) 10	.14	1.6 (1.3-2.2) 10	.13	8.5 (2.1-19.5) 24	.83	8.7 (3.4-15.8) 13	.74	6.7 (5.4-18.2) 11	0.53	9.7 1	.18	10.4 (6.0-14.7) 2	.43
	(–)	4.6 (0.0-20.0) 56		9.6 (2.0-18.2) 21		1.9 (1.2-3.4) 16		6.4 (1.2-21.4) 39		6.6 (2.5-25.2) 12		9.5 (4.5-21.3) 11		9.2 (2.8-9.2) 3		14.0 (9.1-23.5) 8	
Weight loss	(+)	7.0 (2.3-12.8) 10	.04*	6.9 (2.7-20.4) 7	.60	1.5 (1.3-2.4) 6	.36	9.8 (4.1-19.5) 9	.12	8.2 (2.5-18.8) 6	.41	11.9 (5.7-21.3) 5	0.37	9.2 1	.66	12.6 (9.1-16.2) 2	.79
	(–)	4.8 (0.0-20.0) 79		9.6 (1.1-21.9) 24		1.7 (1.2-3.4) 20		6.6 (1.2-21.4) 54		7.0 (3.4-25.2) 19		6.7 (4.5-18.6) 17		9.5 (2.8-9.7) 3		14.0 (6.0-23.5) 8	
Tiredness	(+)	8.4 (2.9-19.0) 9	.03*	7.0 (1.1-13.8) 8	.96	1.7 (1.3-2.7) 6	.90	4.5 (2.7-18.8) 7	.92	9.8 (2.5-18.8) 3	.62	9.3 (6.2-21.3) 4	0.27	9.2 1	.66	9.1 (6.0-16.2) 3	.21
	(–)	4.9 (0.0-20.0) 80		9.6 (1.7-21.9) 23		1.6 (1.2-3.4) 20		7.1 (1.2-21.4) 56		7.3 (3.4-25.2) 22		6.8 (4.5-18.2) 18		9.5 (2.8-9.7) 3		14.1 (11.6-23.5) 7	
Fever	(+)	5.6 (2.3-12.6) 7	.42	9.2 (6.1-21.9) 5	.49	1.3 (1.3-1.4) 5	.005*	14.8 (4.1-19.6) 6	.30	7.5 (4.7-15.8) 5	.42	8.5 (5.7-17.3) 4	0.80	0	—	9.1 1	.23
	(–)	4.9 (0.0-20.0) 82		8.6 (1.1-18.2) 26		1.9 (1.2-3.4) 21		6.4 (1.2-21.4) 57		7.9 (2.5-25.2) 20		7.0 (4.5-21.3) 18		9.3 (2.8-9.7) 4		14.1 (6.0-23.5) 9	

(*Continued*)

Table 1. The Relationship Between the Characteristics of the Patients and the Maximum Standardized Uptake Values of the Pathological Lesions (*Continued*)

Variables		Lung Parenchyma, Median (Range) n	*P*	Pleural, Median (Range) n	*P*	Pleural Effusion, Median (Range) n	*P*	Mediastinal LN, Median (Range) n	*P*	Supraclavicular LN, Median (Range) n	*P*	Intraabdominal LN, Median (Range) n	*P*	Peritoneum, Median (Range) n	*P*	Bone, Median (Range) n	*P*
Hemoptysis	(+)	4.0 (1.3-20.0) 14	.33	5.19 1	1.0	1.9 1	.74	4.8 (2.1-17.9) 8	.32	13.7 (9.8-17.8) 2	.11	12.6 (6.7-18.6) 2	0.30	0	—	6.0 1	.12
	(–)	4.9 (0.0-19.0) 75		8.8 (1.1-21.9) 30		1.6 (1.2-3.4) 25		7.7 (1.2-21.4) 55		7.0 (2.5-25.2) 23		6.8 (4.5-21.3) 20		9.3 (2.8-9.7) 4		14.1 (9.1-23.5) 9	
Pain	(+)	6.4 (1.5-15.6) 23	.13	9.7 (2.7-21.9) 15	.016*	1.6 (1.3-3.4) 13	.74	9.3 (2.1-21.4) 24	.21	9.7 (3.5-18.8) 11	.96	11.2 (5.8-21.3) 10	.01 2*	9.5 (2.8-9.7) 3	.66	13.9 (6.0-16.7) 5	.35
	(–)	4.6 (0.0-20.0) 66		6.3 (1.1-20.4) 16		1.7 (1.2-2.2) 13		6.4 (1.2-21.1) 39		7.3 (2.5-25.2) 14		5.8 (4.5-12.1) 12		9.2 1		14.1 (11.6-23.5) 5	
Night sweat	(+)	5.7 (1.5-19.3) 7	.47	5.4 (1.1-20.4) 3	.29	1.4 1	.32	16.6 (11.9-21.4) 2	.06	5.8 (4.1-7.5) 2	.55	5.7 1	.31	0	—	0	—
	(–)	7.2 (0.0-20.0) 82		8.6 (1.7-21.9) 28		7.7 (1.2-3.4) 25		6.8 (1.2-21.1) 61		8.7 (2.5-25.2) 23		7.3 (4.5-21.3) 21		9.3 (2.8-9.7) 4		14.0 (6.0-23.5) 10	
Dyspnea	(+)	4.9 (2.9-19.0) 21	.92	6.1 (1.1-18.2) 13	.52	1.9 (1.3-3.4) 13	.25	8.1 (2.1-13.1) 13	.63	6.3 (4.5-9.8) 5	.89	7.3 (5.7-11.1) 6	.88	9.5 1	.66	11.6 (6.0-16.7) 4	0.39
	(–)	5.1 (0.0-20.0) 68		10.2 (1.7-21.9) 18		1.5 (1.2-3.1) 13		6.8 (1.2-21.4) 50		8.1 (2.5-25.2) 20		6.7 (4.5-21.3) 16		9.2 (2.8-9.7) 3		14.3 (11.6-23.5) 6	
Symptom number	**1**	4.3 (1.0-15.6) 26		9.3 (3.1-15.7) 8		1.9 (1.6-3.1) 7		5.2 (3.0-18.5) 19		9.2 (3.4-12.3) 4		5.8 (4.9-12.1) 6		2.8 1		14.0 (13.9-14.1) 2	
	2	4.9 (1.3-20.0) 15		10.3 (2.4-21.9) 8		1.5 (1.3-3.4) 6		10.2 (2.7-21.4) 10		4.5 (2.5-17.7) 6		11.2 (7.9-18.6) 5		9.5 (9.2-9.7) 3		16.5 (16.2-16.7) 2	
	3	7.6 (3.1-15.5) 11	.07	9.2 (2.7-13.8) 4	.59	2.2 (1.5-2.7) 5	.15	9.3 (2.7-18.8) 12	.31	10.3 (3.5-18.8) 6	.67	12.8 (6.2-21.3) 4	.05	0	.18	14.7 1	0.21
	4	5.6 (2.9-19.0) 6		2.8 (1.1-4.6) 2		1.35 1		19.5 1		15.8 1		17.3 1		0		0	
	5	6.0 (1.53-10.0) 6		6.1 (5.2-20.4) 4		1.3 (1.3-1.9) 4		8.1 (2.1-18.9) 5		7.5 (6.3-9.8) 3		5.7 (5.7-6.7) 3		0		7.5 (6.0-9.1) 2	

$P < .05$ is considered statistically significant.
*$P < .05$.

Table 2. The Relationship Between the Characteristics of the Patients and the Maximum Standardized Uptake Values of the Lung Parenchymal Lesions

Variables		Consolidation, Median (Range) n	*P*	Cavitation, Median (Range) n	*P*	Micronodule, Median (Range) n	*P*	Nodule, Median (Range) n	*P*
Gender	Female	6.5 (5.3-6.9) 6	.46	4.4 (4.3-7.0) 3	.69	3.2 (1.5-4.9) 2	.44	4.3 (1.0-15.5) 21	.14
	Male	6.6 (2.3-11.3) 15		4.3 (2.9-19.0) 18		4.3 (3.2-5.3) 2		2.8 (0.0-15.6) 46	
Symptom	(+)	6.9 (4.9-11.3) 14	.88	4.6 (2.9-19.0) 15	.35	0	—	2.8 (0.7-15.6) 48	.96
	(−)	6.1 (2.3-8.2) 7		3.9 (3.0-7.0) 6		4.9 (1.5-5.3) 4		3.1 (0.0-7.1) 19	
Sputum	(+)	7.2 (5.8-11.3) 6	.88	6.0 (4.3-7.6) 3	.32	3.4 (1.5-5.3) 2	1.0	4.3 (0.7-15.5) 13	.28
	(−)	6.4 (2.3-8.4) 15		4.3 (2.9-19.0) 18		4.1 (3.2-4.9) 2		2.8 (0.0-15.6) 54	
Cough	(+)	6.4 (4.9-11.3) 7	.50	6.0 (3.4-19.0) 5	.19	3.4 (1.5-5.3) 2	1.0	3.1 (1.0-15.5) 23	.26
	(−)	6.6 (2.3-8.4) 14		4.3 (2.9-11.0) 16		4.1 (3.2-4.9) 2		2.9 (0.0-15.6) 44	
Weight loss	(+)	6.6 (5.8-8.4) 5	.53	6.0 (5.6-8.1) 3	.11	0	—	4.1 (0.7-15.4) 8	.52
	(−)	6.6 (2.3-11.3) 16		4.3 (2.9-19.0) 18		4.9 (1.5-5.3) 4		2.8 (0.0-15.6) 59	
Tiredness	(+)	7.5 (6.6-8.4) 2	.19	12.3 (5.6-19.0)2	.12	0	—	3.8 (1.0-15.4) 6	.21
	(−)	6.6 (2.3-11.3) 19		4.3 (2.9-11.0) 19		4.9 (1.5-5.3) 4		2.8 (0.0-15.6) 61	
Fever	(+)	6.4 (4.9-6.6) 3	.25	4.5 (3.4-5.6) 2	.63	0	—	4.1 (1.3-12.6) 6	.31
	(−)	6.6 (2.3-11.3) 18		4.3 (2.9-19.0) 19		4.9 (1.5-5.3) 4		2.8 (0.0-15.6) 61	
Hemoptysis	(+)	6.2 (5.8-6.6) 2	.63	6.0 (3.1-7.6) 3	.69	3.2 (1.5-4.9) 2	.44	2.0 (0.7-12.8) 8	.25
	(−)	6.6 (2.3-11.3) 19		4.3 (2.9-19.0)18		4.2 (3.2-5.3) 2		3.0 (0.0-15.6) 59	
Pain	(+)	6.6 (4.9-11.3) 8	.97	5.6 (3.4-11.0)6	.35	3.2 (1.5-4.9) 2	.44	2.8 (1.0-15.6) 18	.57
	(−)	6.6 (2.3-8.4) 13		4.3 (2.9-19.0) 15		4.2 (3.2-5.3) 2		3.0 (0.0-12.8) 49	
Night sweat	(+)	7.2 (6.4-8.1) 2	.76	8.1 (2.9-19.0) 3	.42	1.5 1	.18	3.1 (2.1-6.3) 4	.63
	(−)	6.6 (2.3-11.3) 19		4.3 (3.0-11.0) 18		4.9 (3.2-5.3) 3		2.8 (0.0-15.6) 63	
Dyspnea	(+)	6.6 (4.9-6.9) 6	.33	4.8 (3.4-19.0)7	.46	3.2 1	.66	3.0 (0.9-10.9) 17	.56
	(−)	6.6 (2.3-11.3) 15		4.3 (2.9-11.0) 14		4.9 (1.5-5.3) 3		2.8 (0.0-15.6) 50	
Symptom number	1	6.6 (6.5-6.6) 3		4.1 (2.9-11.0)8		3.2 1		2.8 (0.9-15.6) 21	
	2	8.1 (4.9-8.4) 3		6.5 (4.8-8.1) 2		5.1 (4.9-5.3) 2		2.1 (1.0-10.9) 11	
	3	6.9 (5.8-11.3) 3	.59	0	.37	0	.26	3.4 (0.7-15.5) 8	.36
	4	5.6 (4.9-6.4) 2		6.0 (3.6-19.0) 3		0		2.3 (1.0-12.8) 4	
	5	6.6 (6.4-6.6) 3		6.6 (5.6-7.6) 2		1.5 1		5.3 (3.3-6.3) 4	

$P < .05$ is considered statistically significant.
*$P < .05$.

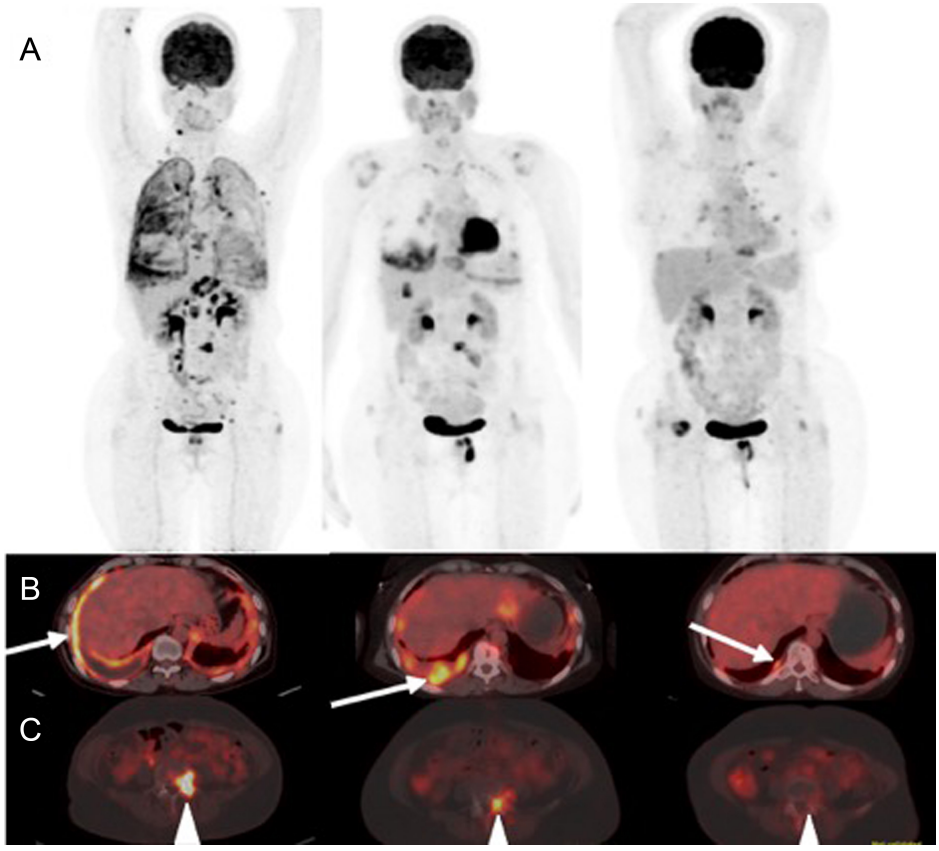

Figure 1. 18-F FDG PET/CT scan showing EP TB in a 43-year-old female patient. Initial and after anti-TB treatment control PET studies are shown (left to right columns). Whole-body maximum intensity projection images are shown (A). Trans-axial fused images showing FDG-avid pleural (B; arrows) and bone lesions (C; arrowheads) regression after anti-TB treatment. CT, computed tomography; EP, extrapulmonary; 18-F FDG, fluoro-2-deoxy-D-glucose; FDG, fluorodeoxyglucose; PET, positron emission tomography; TB, tuberculosis.

values of the pleural lesions and the ages of the cases ($r = -0.43$, $P = .02$). There was no significant correlation between *SUV*max values of other lesions with age and number of symptoms.

Some examples of our cases are shown in Figures 1, 2, 3, and 4.

Discussion

Two patterns of FDG-avid active P TB have been described:[6,7] (1) The lung pattern presents with predominantly P symptoms. In lesions seen in milder forms of TB, 18-F FDG uptake is usually low to moderate and (2) The lymphatic pattern is related to a systemic infection and presents with systemic symptoms. The main finding is more enlarged mediastinal and hilar lymph nodes with higher FDG uptake than lung pattern. In our study, while lung parenchymal involvement was significantly higher in males, hypermetabolic lymph nodes in all localizations were found significantly more in females. However, there was no significant difference in symptom status between the genders.

Contrary to the literature, we did not find a significant difference between the *SUV*max value of any lesion in symptom-positive and -negative groups.[8] However, this study was conducted with a small cohort of 57 subjects. The *SUV*max value was not categorized for different types of lesions and only the *SUV*max values of PET-positive lesions were measured.

Typically, parenchymal disease manifests as consolidation, with predominance in the lower and middle lobes.[9] Our cohort superior lobe involvement was significantly higher than multilobar involvement. No significant difference was detected between the involvement of other lobes. As expected because it represents a more severe disease, *SUV*max values of patients with multilobar involvement were found to be significantly higher than those with superior lobe involvement.

Although consolidation is accepted as the most common radiographic manifestation of TB, we detected nodules more than consolidation, but the difference was not statistically significant.[10,11] This difference is probably due to the higher indication rate of FDG PET for the metabolic characterization of the nodules in the cases.

Cavitation, the radiological hallmark of P TB, is radiographically evident in 20%-45% of patients.[10,11] In our series, this rate was 18.4%. Interestingly, ratios of cavitation-positive cases were similar in symptom-positive and -negative cases (17.9% vs. 20.0%).

As expected, *SUV*max values of lung lesions increase with symptom number. Both of these parameters reflect aggressive disease. Goo et al[12] found a mean *SUV*max of 4.2 mg/dL in histopathologically proven P tuberculomas in 9 of 10 consecutive patients. In our study, the highest *SUV*max value was measured in consolidation as 6.6 mg/dL. However, *SUV*max values did not differ significantly with types of lung lesions.

In the immunosuppressed population, EP TB cases can be seen at a rate of 50% and above. However, it is usually seen in 20% of cases in the normal population.[13] 18-Fluorine fluoro-2-deoxy-D-glucose positron emission tomography/computed tomography is especially valuable in terms of identification of EP involvement sites like central nerve, and skeletal systems which require a longer duration of anti-TB treatment.[14,15] In symptom-positive and -negative patient groups, there was no significant difference

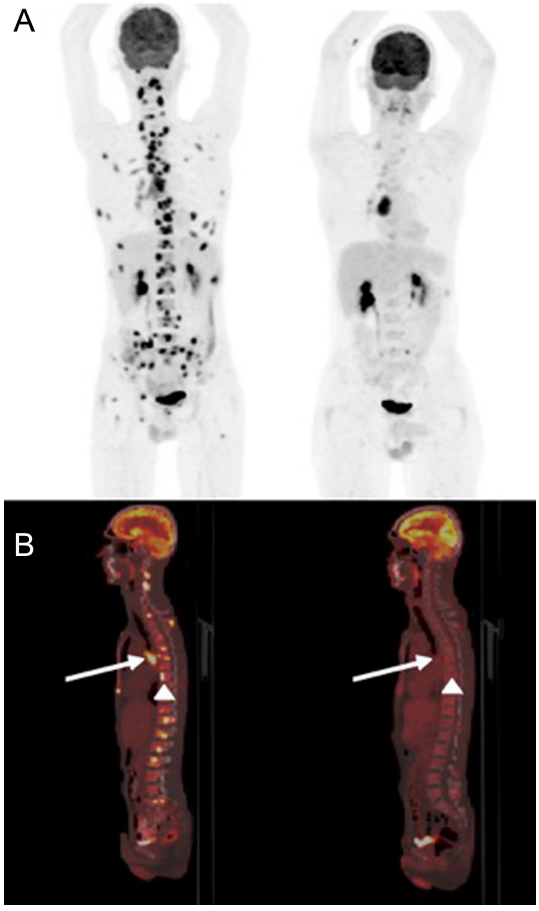

Figure 2. 18-F FDG PET/CT scan showing EP TB in a 32-year-old male patient. Initial and after anti-TB treatment control PET studies are shown (left-to-right columns). Whole-body maximum intensity projection images are shown (A). Trans-sagittal-fused images showing FDG-avid subcarinal lymph node (B; arrows) and bone lesions (B; arrowheads) regression after anti-TB treatment. CT, computed tomography; EP, extrapulmonary; 18-F FDG, fluoro-2-deoxy-D-glucose; FDG, fluorodeoxyglucose; PET, positron emission tomography; TB, tuberculosis.

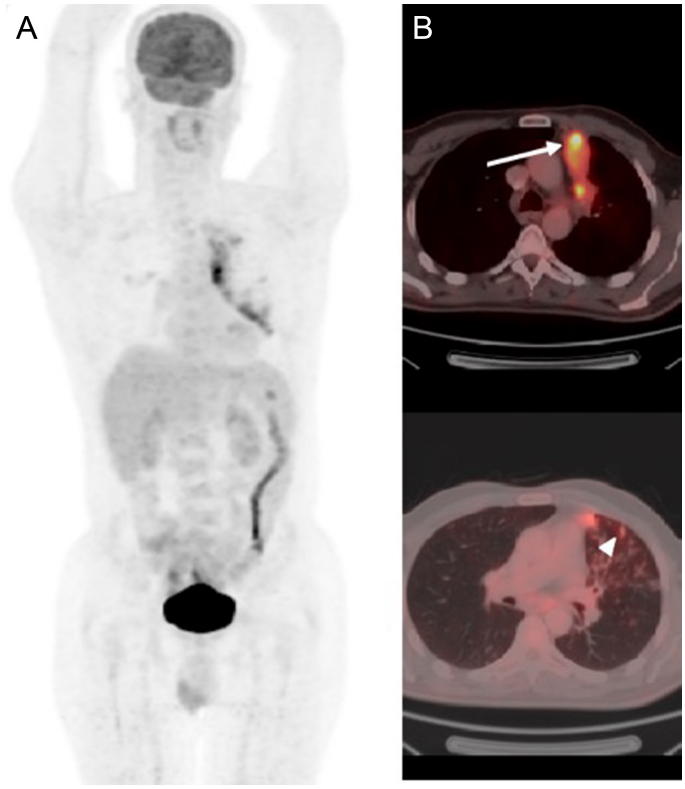

Figure 3. 18-F FDG PET/CT scan showing pulmonary TB in a 51-year-old male patient. Whole-body maximum intensity projection images are shown (A). Trans-axial fused images showing FDG-avid consolidation (B; arrow), and reticulonodular opacities (B; arrowhead). CT, computed tomography; 18-F FDG, fluoro-2-deoxy-D-glucose; FDG, fluorodeoxyglucose; PET, positron emission tomography; TB, tuberculosis.

in EP involvement sites. Fluoro-2-deoxy-D-glucose positron emission tomography/computed tomography did not reveal EP lesions in cases with inactive disease. This is an important finding that guides the decision to start treatment in cases with EP lesions. In symptom-positive and -negative cases, the *SUV*max value of EP lesions did not differ significantly. This finding could be attributed to low EP lesions number.

Pleural effusion can be present in up to 18%-25% of the patients with P TB.[16] Consistent with this data, the pleural effusion rate was 22.8% in our study. Coexistence of pleural effusion and pleural pathology was not detected in most of the cases (pleura+ effusion−: 41.9%, n = 13; pleura− effusion+: 33.9%, n =7). According to *SUV*max values, only 6.5% (n = 2) of pleural lesions were inactive, but as expected, this rate was as high as 69.2% (n = 18) in effusion. We detected higher *SUV*max values in pleural involvement in young-age cases. Especially, in young age, aggressive pleural involvement should be suspected.

Musculoskeletal TB frequently involves the spine.[9] Spondylodiscitis, also known as Pott's disease, is the most common form.[17] 18-Fluorine fluoro-2-deoxy-D-glucose positron emission tomography is a promising technique for diagnosing spinal infection. It has a high sensitivity in lesion detection and unlike magnetic resonance imaging, image quality is not affected by metal artifacts.[18-20] FDG PET detected bone marrow involvement in 6 cases, and lesions were consistent with spondylodiscitis in 4 cases. While 50% of the cases with spondylodiscitis presented with pain complaints; *SUV*max values of symptom-positive and symptom-negative cases with bone lesions were similar. However, this result could be related to small cohort with bone lesions.

Abdominal LN is the most common manifestation of abdominal TB, seen in 55%-66% of patients.[21] In 81.8% of our cases, pathologic abdominal LN did not associate with other abdominal organ involvement.

One of the details indicating the risk of developing active TB is that the balance between the host's immune response and the proliferating bacillus can be demonstrated in metabolically active old TB lesions. As the SUV max values detected in patients with healed old TB lesions increase, a higher risk of active TB can be mentioned.[22] Consistent with the literature, we found a high rate of active lesions in the symptom-negative group (80% vs. 70.4%).[8] These findings are very important in terms of clinical follow-up, and planning FDG PET imaging even in asymptomatic cases.

The inability to demonstrate histopathological verification for all detected lesions and the retrospective design stands out as the limitations of this study.

Observation of 18-F FDG uptake in granulomatous diseases such as sarcoidosis, toxoplasmosis, and non-specific inflammatory lymphadenopathy is due to the pathological involvement of 18-F

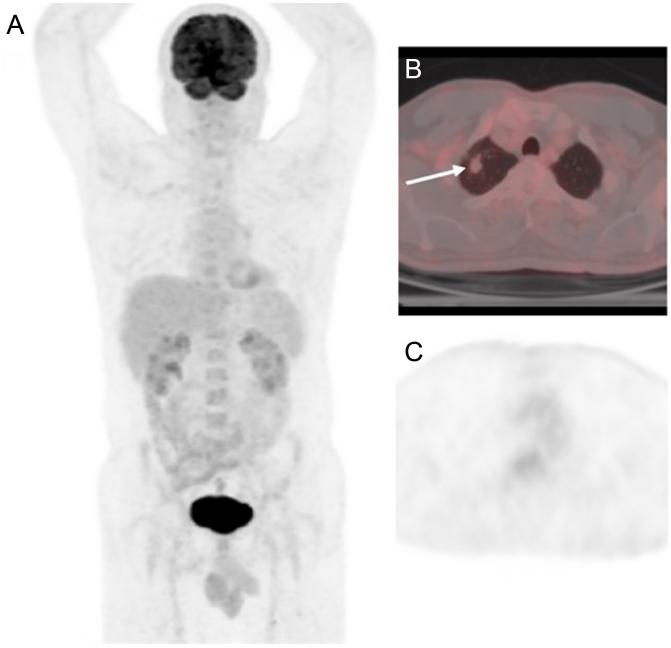

Figure 4. A 61-year-old male patient with pulmonary TB history underwent 18-F FDG PET/CT scan for metabolic characterization of right lung apical segment located nodules. Whole-body maximum intensity projection images are shown (A). Trans-axial fused (B) and PET (C) images showing non-FDG-avid nodules (arrow). CT, computed tomography; 18-F FDG, fluoro-2-deoxy-D-glucose; FDG, fluorodeoxyglucose; PET, positron emission tomography; TB, tuberculosis.

FDG in both inflammatory and malignant processes. Therefore, 18-F FDG is a non-specific tracer. Because both pathologies show high FDG affinity, 18-F FDG PET ability to differentiate TB from malignancy is limited.[23] The value of dual time point imaging in this setting remains controversial.[24-27] Clinically, diagnosis should be confirmed bacteriologically and/or histopathologically not to skip possible malignancy.

One of the potentially most important clinical applications in TB is the evaluation of treatment response with the 18-F FDG PET/CT imaging modality. While molecular changes are observed in the early period, morphological changes take longer to be observed. Promising results have also been obtained with the use of other radioactive agents. Among these agents, 11-C choline,[28-30] 18-F Fluoro thymidine,[31,32] and 68-Ga citrate have been reported.

Conclusion

18-Fluorine fluoro-2-deoxy-D-glucose positron emission tomography/computed tomography is a valuable, noninvasive, whole-body imaging modality in TB staging and localizing EP TB, and assessing early treatment response. It can reliably differentiate active from inactive disease. In our study, we did not detect any significant difference between symptom-positive and -negative cases in terms of localization and types of lesions. Only a low correlation was detected between SUVmax and a number of symptoms. Fluoro-2-deoxy-D-glucose positron emission tomography revealed active disease even in the majority of asymptomatic cases. For these reasons, we would like to state that active or inactive TB should not be defined solely on the basis of clinical symptoms. Fluoro-2-deoxy-D-glucose positron emission tomography reliably distinguishes between active and inactive disease before anatomic imaging modalities. Problems such as misdiagnosis and delayed treatment may be more common in asymptomatic TB cases. It is necessary to focus more on the clinical status in these cases. Early initiation of treatment together with early and accurate diagnosis is the key factor in minimizing morbidity and mortality in TB patients. In addition, the possibility of transmission is prevented.

Ethics Committee Approval: Ethical committee approval was received from the Ethics Committee of University of Yedikule Chest Diseases and Thoracic Surgery Training and Research Hospital (Date: January 1, 2023, Number: 2023/313).

Informed Consent: Informed consents were not required for retrospective review of the medical and radiological data of the patients.

Peer-review: Externally peer-reviewed.

Author Contributions: Concept – E.A., R.A.; Design – E.A., R.A.; Supervision – E.A.; Resources – E.A., R.A.; Materials – E.A., R.A.; Data Collection and/or Processing – E.A., R.A.; Analysis and/or Interpretation – E.A.; Literature Search – E.A., R.A.; Writing Manuscript – E.A.; Critical Review - E.A.

Declaration of Interests: The authors have no conflict of interest to declare.

Funding: The authors declared that this study has received no financial support.

References

1. World Health Organization. Global tuberculosis report 2022. Available at: https://www.who.int/publications/i/item/9789241565714
2. Cohen A, Mathiasen VD, Schön T, Wejse C. The global prevalence of latent tuberculosis: a systematic review and meta-analysis. *Eur Respir J*. 2019;54(3):1900655. [CrossRef]
3. Lawn SD, Zumla AI. Tuberculosis. *Lancet*. 2011;378(9785):57-72. [CrossRef]
4. Behera D. *Textbook of Pulmonary Medicine*. 2nd ed. New Delhi: Jaypee Brothers Medical Publishers; 2010.
5. Heysell SK, Thomas TA, Sifri CD, Rehm PK, Houpt ER. 18-fluorodeoxyglucose positron emission tomography for tuberculosis diagnosis and management: a case series. *BMC Pulm Med*. 2013;13:14. [CrossRef]
6. Skoura E, Zumla A, Bomanji J. Imaging in tuberculosis. *Int J Infect Dis*. 2015;32:87-93. [CrossRef]
7. Soussan M, Brillet PY, Mekinian A, et al. Patterns of pulmonary tuberculosis on FDG-PET/CT. *Eur J Radiol*. 2012;81(10):2872-2876. [CrossRef]
8. Yu WY, Zhang QQ, Xiao Y, Tan WG, Li XD, Lu PX. Correlation between 18F-FDG PET CT SUV and symptomatic or asymptomatic pulmonary tuberculosis. *J X-Ray Sci Technol*. 2019;27(5):899-906. [CrossRef]
9. Burrill J, Williams CJ, Bain G, Conder G, Hine AL, Misra RR. Tuberculosis: a radiologic review. *RadioGraphics*. 2007;27(5):1255-1273. [CrossRef]
10. Leung AN. Pulmonary tuberculosis: the essentials. *Radiology*. 1999;210(2):307-322. [CrossRef]
11. Krysl J, Korzeniewska-Kosela M, Müller NL, FitzGerald JM. Radiologic features of pulmonary tuberculosis: an assessment of 188 cases. *Can Assoc Radiol J*. 1994;45(2):101-107.
12. Goo JM, Im JG, Do KH, et al. Pulmonary tuberculoma evaluated by means of FDG PET: findings in 10 cases. *Radiology*. 2000;216(1):117-121. [CrossRef]
13. Ramírez-Lapausa M, Menéndez-Saldaña A, Noguerado-Asensio A. Extrapulmonary tuberculosis. *Rev Esp Sanid Penit*. 2015;17(1):3-11. [CrossRef]
14. Sood A, Mittal BR, Modi M, et al. 18F-FDG PET/CT in tuberculosis: can interim PET/CT predict the clinical outcome of the patients? *Clin Nucl Med*. 2020;45(4):276-282. [CrossRef]
15. World Health Organization. Treatment of tuberculosis [guidelines] 2022. Available at: http://www.who.int/iris/handle/10665/44165.
16. Jeong YJ, Lee KS. Pulmonary tuberculosis: up-to-date imaging and management. *AJR Am J Roentgenol*. 2008;191(3):834-844. [CrossRef]

17. Martini M, Ouahes M. Bone and joint tuberculosis: a review of 652 cases. *Orthopedics*. 1988;11(6):861-866. [CrossRef]
18. Skaf GS, Domloj NT, Fehlings MG,et al. Pyogenic spondylodiscitis: an overview. *J Infect Public Health*. 2010;3(1):5-16. [CrossRef]
19. Kälicke T, Schmitz A, Risse JH, et al. Fluorine-18 fluorodeoxyglucose positron emission tomography in infectious bone diseases: results of histologically confirmed cases. *Eur J Nucl Med*. 2000;27(5):524-528. [CrossRef]
20. Guhlmann A, Brecht-Krauss D, Suger G, et al. Chronic osteomyelitis: detection with FDG PET and correlation with histopathologic findings. *Radiology*. 1998;206(3):749-754. [CrossRef]
21. Leder RA, Low VH. Tuberculosis of the abdomen. *Radiol Clin North Am*. 1995;33(4):691-705. [CrossRef]
22. Jeong YJ, Paeng JC, Nam HY, et al. (18)F-FDG positron-emission tomography/computed tomography findings of radiographic lesions suggesting old healed tuberculosis. *J Korean Med Sci*. 2014;29(3):386-391. [CrossRef]
23. Vesselle H, Salskov A, Turcotte E, et al. Relationship between non-small cell lung cancer FDG uptake at PET, tumor histology, and Ki-67 proliferation index. *J Thorac Oncol*. 2008;3(9):971-978. [CrossRef]
24. Suga K, Kawakami Y, Hiyama A, et al. Dual-time point 18F-FDG PET/CT scan for differentiation between 18F-FDG-avid nonsmall cell lung cancer and benign lesions. *Ann Nucl Med*. 2009;23(5):427-435. [CrossRef]
25. Kim DW, Park SA, Kim CG. Dual-time-point positron emission tomography findings of benign mediastinal fluorine-18-fluorodeoxyglucose uptake in tuberculosis-endemic region. *Indian J Nucl Med*. 2011;26(1):3-6. [CrossRef]
26. Barger RL Jr, Nandalur KR. Diagnostic performance of dual-time 18F-FDG PET in the diagnosis of pulmonary nodules: a meta-analysis. *Acad Radiol*. 2012;19(2):153-158. [CrossRef]
27. Cloran FJ, Banks KP, Song WS, Kim Y, Bradley YC. Limitations of dual time point PET in the assessment of lung nodules with low FDG avidity. *Lung Cancer*. 2010;68(1):66-71. [CrossRef]
28. Liu Q, Peng ZM, Liu QW, et al. The role of 11C-choline positron emission tomography-computed tomography and videomediastinoscopy in the evaluation of diseases of middle mediastinum. *Chin Med J (Engl)*. 2006;119(8):634-639. [CrossRef]
29. Hara T, Inagaki K, Kosaka N, Morita T. Sensitive detection of mediastinal lymph node metastasis of lung cancer with 11C-choline PET. *J Nucl Med*. 2000;41(9):1507-1513.
30. Hara T, Kosaka N, Suzuki T, Kudo K, Niino H. Uptake rates of 18F-fluorodeoxyglucose and 11C-choline in lung cancer and pulmonary tuberculosis: a positron emission tomography study. *Chest*. 2003;124(3):893-901. [CrossRef]
31. Yamamoto Y, Nishiyama Y, Kimura N, et al. Comparison of (18) F-FLT PET and (18)F-FDG PET for preoperative staging in nonsmall cell lung cancer. *Eur J Nucl Med Mol Imaging*. 2008;35(2):236-245. [CrossRef]
32. Yang W, Zhang Y, Fu Z, et al. Imaging of proliferation with 18F-FLT PET/CT versus 18F-FDG PET/CT in nonsmall-cell lung cancer. *Eur J Nucl Med Mol Imaging*. 2010;37(7):1291-1299. [CrossRef]